Electronic Supplementary Information (ESI)

Reusable nanofibrous film chemosensor for highly selective and sensitive optical signaling of Cu^{2+} in aqueous media

Wei Wang,[a] Xiuling Wang,[a] Qingbiao Yang,[a]* Xiaoliang Fei,[a] Mingda Sun[a] and Yan Song [b]*

[a] Department of Chemistry, Jilin University, Changchun, 130021, People's Republic of China.

[b] Department of Chemical and Materials Engineering, Jilin Institute of Chemical Technology, Jilin, 132022, People's Republic of China.

1. Experimental

1.1. Materials: Rhodamine B (RhB) and 2,4-Dihydroxybenzaldehyde were purchased from Sigma-Aldrich. Acryloyl chloride, hydrazine hydrate (85%), triethylamine and hydroquinone were obtained from Alfa. Rhodamine B (RhB, 99%) was obtained from Acros Organics. All the reagents and inorganic metal salts with analytical grade (Shanghai Chemical Reagents Co. China) were used without further purification. The solutions of metal ions were prepared from NaCl, KCl, $CaCl_2$, $MgSO_4$, $FeCl_3$, $Mn(NO_3)_2{\cdot}6H_2O$, $CoCl_2{\cdot}6H_2O$, $NiCl_2{\cdot}6H_2O$, $Zn(NO_3)_2$, $CdCl_2$, $CuCl_2{\cdot}2H_2O$, $HgCl_2$, $AgNO_3$, $Pb(NO_3)_2$ respectively, and were dissolved in deionized water. Aqueous HEPES-NaOH (0.1 mol L^{-1}) solution was used as buffer to keep pH value (pH=7. 20), and to maintain the ionic strength of all solutions in experiments.

1.2. Characterization: The fluorescent unit of rhodamine B-hydrazine (RhB-hydrazine) was first prepared via the established literature procedure. 2,4-Dihydroxybenzaldehyde was functionalized with acryloyl chloride to gain the corresponding monomer 4-aldehyde-3-hydroxy phenyl acrylate (AHPA) (Scheme S1). Then poly (MMA-co-AHPA) was prepared by free-radical copolymerization of AHPA and methyl methacrylate (MMA) in anhydrous solution of N,N-Dimethylformamide (DMF) with 2,2-azobis(isobutyronitrile) (AIBN) as an initiator. Following, continuous fibers were obtained from the electrospinning of 22 wt % poly (MMA-co-AHPA)/DMF solution. Finally, since the surface of the poly (MMA-co-AHPA) nanofibrous film contains large amount of aldehyde groups, the surface modification was carried out easily in anhydrous ethanol solution. In this

reaction solution Rh6B-hydrazine fluorophores could dissolve, thus allowing the amino groups of the fluorophores react with the aldehyde groups on the surface of film. The resulting molar ratio of RhB and poly(MMA-co-AHPA) units in the nanofibrous film was 1:3535, derived from spectral results or standard Job's plot of RhB-Cu absorption spectra in DMF (excitation at 555 nm).

^{1}H NMR spectra were measured on a Bruker AV-400 spectrometer with chemical shifts reported as parts per million (in $CDCl_3$, TMS as internal standard). The pH values of the test solutions were measured with a glass electrode connected to a Mettler-Toledo Instruments DELTA 320 pH meter (Shanghai, China) and adjusted if necessary. FTIR spectra of the products were recorded on a Perkin-Elmer Paragon1000 FTIR spectrometer. Absorption and luminescence spectra were studied on a Shimadzu UV 2100 PC UV-visible spectrophotometer and a Hitachi F-4500 luminescence spectrometer, respectively. The surface areas were measured using a Micromeritics ASAP 2010 Brunauer-Emmett-Teller BET surface analysis apparatus with N_2 gas.

1.3. Synthesis of rhodamine B-hydrazine (RhB-hydrazine): Rhodamine B (5g, 10.46mmol) was dissolved in 150mL of anhydrous ethanol; 10 mL (excess) hydrazine hydrate (85%) was then added. After the addition, the stirred mixture was heated to reflux in an air bath for 2 h. The solvent was evaporated under reduced pressure, 1 M NaOH was added slowly with stirring until the pH of the solution reached 9–10. The resulting precipitate was filtered and washed 3 times with water. The crude material was purified by flash column chromatography to give white product RhB-hydrazine.

(CH_2Cl_2/EtOH/ Et_3N, 5:1:0.1) Yield: 62.8%. ^{1}H NMR (300 MHz, $CDCl_3$, δ): 7.93 (dd, *J* = 5.6, 3.1 Hz, 1H; Ar H), 7.57 – 7.34 (m, 1H; Ar H), 7.32 – 7.18 (m, 2H; Ar H), 7.14 – 7.01 (m, 2H; Ar H), 6.43 (dd, *J* = 12.3, 5.5 Hz, 2H; Ar H), 6.33 – 6.20 (m, 2H; Ar H), 3.80 – 3.64 (m, 2H; NH_2), 3.33 (q, *J* = 7.0 Hz, 8H; CH_2), 1.32 – 1.07 (m, 12H; CH_3); IR (KBr): *v* = 3428 (s; $\nu_{as}(NH_2)$), 2966 (m; (ν_{as}(CH)), 2925 (m; ν_s(CH)), 2849 (m; ν_{as}(CH)), 1689 (s), 1623 (s; ρ(N-H)), 1510 (s; σ(N-N)), 1452 (m), 1421 (m; ρ(CH)), 1292 (m), 1266 (s), 1216 (s; ν_s(Ar-OH)), 1148 (m; ν_{as}(C-N)), 1010 (w; ν_{as}(C-O-C)), 981 (m; ν_s(C-O-C)), 744 cm^{-1} (s; ω(Ar-CH)); HRMS (ESI, *m/z*): [*M* + H]$^+$ calcd for $C_{28}H_{32}N_4O_2$, 456.25; found, 457.3.

1.4. Synthesis of 4-aldehyde-3-hydroxy phenyl acrylate (AHPA): AHPA was prepared via the established literature procedure.[1] 2,4-Dihydroxybenzaldehyde (6.90 g, 0.05 mol), triethylamine (6.8 mL, 0.05 mol), and hydroquinone (1.50 g) were mixed in 2-butanone (500 mL) were taken necked flask and the contents cooled to 0 ℃. Acryloyl chloride (4.5 mL in 25mL of 2-butanone) was added dropwise with constant stirring at that temperature. The reaction mixture was gradually allowed to attain room temperature and stirring continued for 2 h. The byproduct, quaternary ammonium salt, formed was filtered off. The filtrate was thoroughly washed with distilled water, dried over anhydrous MgSO4. The solvent was evaporated under vacuum to obtain an oil product. The final white block crystals were recrystallized from ethanol/water mixture. Yield: 62.79% (6.03 g). ^{1}H NMR (300 MHz, $CDCl_3$, δ): 9.91 (d, *J* = 24.2 Hz, 1H; CHO), 7.59 (d, *J* = 8.4 Hz, 1H; Ar H), 7.26 (t, *J* = 2.1 Hz, 1H; Ar H), 6.96 – 6.73 (m, 1H; Ar H), 6.64 (dd, *J* = 17.3, 0.8 Hz, 1H; CH=CH_2), 6.42

– 6.22 (m, 1H; CH=CH_2), 6.07 (dd, J = 10.4, 0.8 Hz, 1H; CH=CH_2), 5.30 (d, J = 0.7 Hz, 1H; Ar-OH); IR (KBr): ν = 3400(w, ν_{as}(Ar-OH)), 3102 (w; ν_s(CH)), 1750 (s; ν_{as}(C=O)), 1670 (s, ν_{as}(CHO)), 1375 (m), 1436 (m), 1149 (s, ν_s(Ar-OH)), 981 (w), 800 cm^{-1} (m; ω(CH=CH_2)); HRMS (ESI, *m/z*): $[M + H]^+$ calcd for $C_{10}H_8O_4$, 192.04; found, 193.0.

1.5. Synthesis of poly (MMA-co-AHPA) (PMA): Poly (MMA-co-AHPA) was prepared by the copolymerization of AHPA and MMA with AIBN as a thermal initiator. Briefly, 1.9 g (0.01 mol) AHPA, 2.0 g (0.02 mol) of MMA, and 0.02 g (0.01 mol) of AIBN in 10mL of DMF were introduced into a dry polymerization tube. The solution was deoxygenated by purging with N_2 gas for 5min. The tube was sealed and placed in a regulated thermostat bath at 70 ℃ for 24 h. The obtained poly (MMA-co-AHPA) was transparent and colourless. It was dissolved in $CHCl_3$ (20 mL) and precipitated with CH_3OH (200 mL). After successive dissolving and precipitation (5 times), the colored PMMA was filtrated on a glass filter and dried under vacuum at 50 ℃ to a constant weight.

1.6. Preparation of poly (MMA-co- AHPA) nanofibrous film (PMA nanofibrous film): Poly (MMA-co-AHPA) of 1 g was added to 3.5 g DMF solution to prepare precursor solution with a concentration of 22 wt%. The solution was rapidly stirred for 24 h at room temperature. The resulting clear homogenous solution was used for electrospinning the film. A burette with an inserted Cu rod to connect the high-voltage supply was filled with the precursor solution. An aluminum foil served as the counter electrode. The distance between the burette tip and receiver was fixed at 17 cm. The

high-voltage supply was fixed at 15 kV. The spinning rate was controlled at about 4 mL/h by adjusting the angle of inclination of the burette. The electrospinning was performed at 25 ℃.

1.7. Synthesis of poly (MMA-co- AHPA)/RhB multifunctional nanofibrous film (PMAR nanofibrous film): Poly (MMA-co-AHPA) nanofibrous film (size: 15 cm × 10 cm, weight: 0.5760±0.002 g) was allowed to react with RhB-hydrazine (1.00 g, 2.19 mmol) in dry ethanol (100 mL) at 100 ℃ for 12 h. The product was repeatedly washed with toluene, and then extracted in a Soxhlet extractor with ethanol for 6 h for the removal of excess RhB-hydrazine. The final product was vacuum dried at 25 ℃.

Preparation of the fluorometric copper ion titration solution: Procedures for metal-ion sensing: Stock solutions of the copper ions (1.0×10^{-4} mol L^{-1}) were prepared in deionized water, and was then diluted to (1.0×10^{-6} molL^{-1}-2.0×10^{-4} mol L^{-1}) with EtOH-H_2O (0.01 M, HEPES-NaOH buffer at pH 7.2, 1:1, v/v) solution. Titration experiments were performed by placing 4.0 mL of a solution of Cu^{2+} (1.0×10^{-6}-2.0×10^{-5} mol L^{-1}) in a standard 1 cm square fluorometer cells, and then the PMAR nanofibrous film (size: 1.4 cm × 4.0 cm, weight: 0.0245±0.0005 g) was added to the standard fluorlmeter cells of Cu^{2+} solution for fluorescence spectra measurement. All test solutions were slowly stirred for 1 min and then allowed to stand at room temperature for 30 min. For fluorescence measurements, excitation wavelength was provided at 525 nm, and emission spectra were collected from 530 to 700 nm. Both excitation and emission slit widths were set to be either 2.5 or 5 nm.

2. The molar ratio of poly (MMA-co-AHPA) and RhB units in the copolymer

composition.

The value of m / n = 3535 / 1 in PMAR can be calculated standard Job's plot of RhBCu absorption spectra in ethanol solution. From Figure S4, the standard Job's plot of RhBCu (λ_{abs} = 560 nm) is fitted as Equation (1):

$$Y_{Abs} = 0.01573 + 0.05565 \times C_{RhBCu} \quad (1)$$

$$M_{poly\ (MMA\text{-}co\text{-}AHPA)/RhBCu} = M_{poly\ (MMA\text{-}co\text{-}AHPA)} + M_{RhBCu} \quad (2)$$

Based on Figure S3, the absorbance of 1.0 g/L poly (MMA-co-AHPA)/RhBCu at 555 nm is 0.1729, then for the resulting copolymer, the chromophore RhB (C_{RhBCu}) is 2.82 $\times 10^{-6}$ M, that is, $M_{RhB} = 1.76 \times 10^{-3}$ g/L. Therefore:

$$M_{poly(HEMA\text{-}co\text{-}DCPDP)} = M_{poly(HEMA\text{-}co\text{-}DCPDP)/RhB} - M_{RhB} = 0.9982\ g/L \quad (3)$$

$$C_{poly(HEMA\text{-}co\text{-}DCPDP)} = 9.97 \times 10^{-3}\ M \quad (4)$$

$$m / n = C_{poly(HEMA\text{-}co\text{-}DCPDP)} / C_{RhB} = 3535 / 1 \quad (5)$$

3. Adsorption kinetics of Cu^{2+} ions onto PMAR nanofibrous film.

Fig. S6a illustrates the equilibrium adsorption amounts at 24 h under various equilibrium concentrations. It was found that the adsorption amount of metal ions increased with increasing initial ion concentration then reached a plateau value at higher concentration. The initial increase might be due to the high surface area, many available binding sites on the PMAR nanofibrous film [2] and the chelating sites of the reactive fiber become saturated when the metal ion concentration is reached at 200 ppm. The concentration of Cu^{2+} ions in aqueous solution was determined by inductively coupled plasma mass spectrometry (ICP-MS). The adsorption equilibrium data of Cu^{2+} ions were analyzed with the following Langmuir adsorption equation [3],

Freundlich [4], and Temkin and Pyzhev [5] isotherm models were used (Eqs. (1) - (3)).

The linear form of the Langmuir isotherm is given by

$$\frac{C_e}{q_e} = \frac{1}{K_L q_m} + \frac{C_e}{q_m} \quad (1)$$

where C_e (mg L^{-1}) and q_e (mg g^{-1}) are the amount of ions remained in the solution and adsorbed onto the reactive fiber at equilibrium, respectively, q_m (mg g^{-1}), and K_L (L mg^{-1}) are the Langmuir constants related to the saturation adsorption capacity and binding energy (affinity), respectively.

The Freundlich equation is given by

$$\ln q_e = \ln K_F + \frac{\ln C_e}{n} \quad (2)$$

where both K_F and n are constants.

The Tempkin isotherm has been used in the following form:[5]

$$q_e = \left(\frac{RT}{b}\right) \ln A + \left(\frac{RT}{b}\right) \ln C_e \quad (3)$$

where $B = RT/b$.

A plot of q_e versus ln C_e enables the determination of the constants A and B. The constant B is related to the heat of adsorption.

The results obtained from adsorption isotherms for Cu^{2+} ions by PMAR nanofibrous film are shown in Table S1. For the three studied systems, the Langmuir isotherm showed more significant correlation ($R^2 > 0.99$) than in case of Freundlich and Tempkin isotherm with the experimental data from adsorption equilibrium of metal ions by PMAR nanofibrous film suggested a monolayer adsorption. The basic assumption of the Langmuir theory is that adsorption takes place at specific

homogeneous sites within the adsorbent and once a metal ion occupies a reaction site, then no further adsorption occurs at that location. Thus, monolayer adsorption happened on the PMAR nanofibrous film [6-8]. The values of q_m and K_L in Table 1 were calculated from the slope and intercept of the C_e/q_e versus C_e plot in Fig. S6b. The linear plot indicates that Cu^{2+} ion adsorption followed the Langmuir isotherm. The basic assumption of the Langmuir theory is that adsorption takes place at specific homogeneous sites within the adsorbent.

4. Proposed mechanism

According to the molecular structure and spectral results of fluorophore moiety, it is concluded that Cu^{2+} ion could chelate with the imine N, carbonyl O and phenol O atoms of fluorophore moiety, [9-11] resulting in the spirolactam ring open and concomitant formation of fluorophore moiety-Cu^{2+} complex, similar to the previously reported.[12] Finally, a stable cyclic product is formed (Fig. S12). The spirolactam moiety of the rhodamine group act as a signal switcher, which is envisioned to turn on when the cation is bound.[13] It demonstrates that PMAR nanofibrous film can sensitively detect Cu^{2+} with high selectivity over other interfering metal ions.

5. Effect of media

In pure aqueous solution, the fluorescence intensity of PMAR nanofibrous film with the addition of Cu^{2+} ions were lower, which might be due to the poor solubility of the fluorophore moiety in water. On the other hand, when the fluorescence of PMAR-Cu^{2+} is measured in ethanol-water solution, a strong fluorescence signal is obtained. To obtain a more optimal condition for the chemosensing of Cu^{2+}, the effect of ethanol content on the fluorescence signal of PMAR-Cu^{2+} is studied in the range 0-90% (v/v), and the results is shown in Fig. S13. From Fig. S13, it can be seen that the fluorescence intensity increases with increasing the ethanol content and reaches a stable signal when ethanol content is about 50% (v/v). Based on the above results, ethanol-water (1:1, v/v) solution is chosen for fluorescence assay in subsequent experiment.

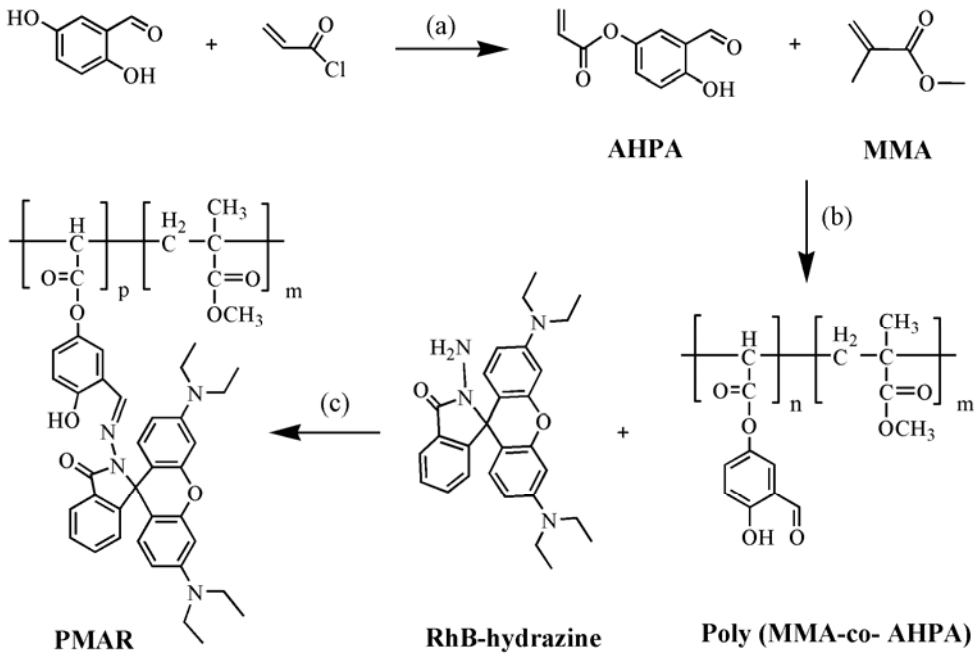

Scheme S1 Synthesis procedures of AHPA and PMAR. (a) TEA, 2-butanone, 0-5℃, 2h; (b) AIBN, DMF, 70℃, 24h; (c) Ethanol, reflux, 12h.

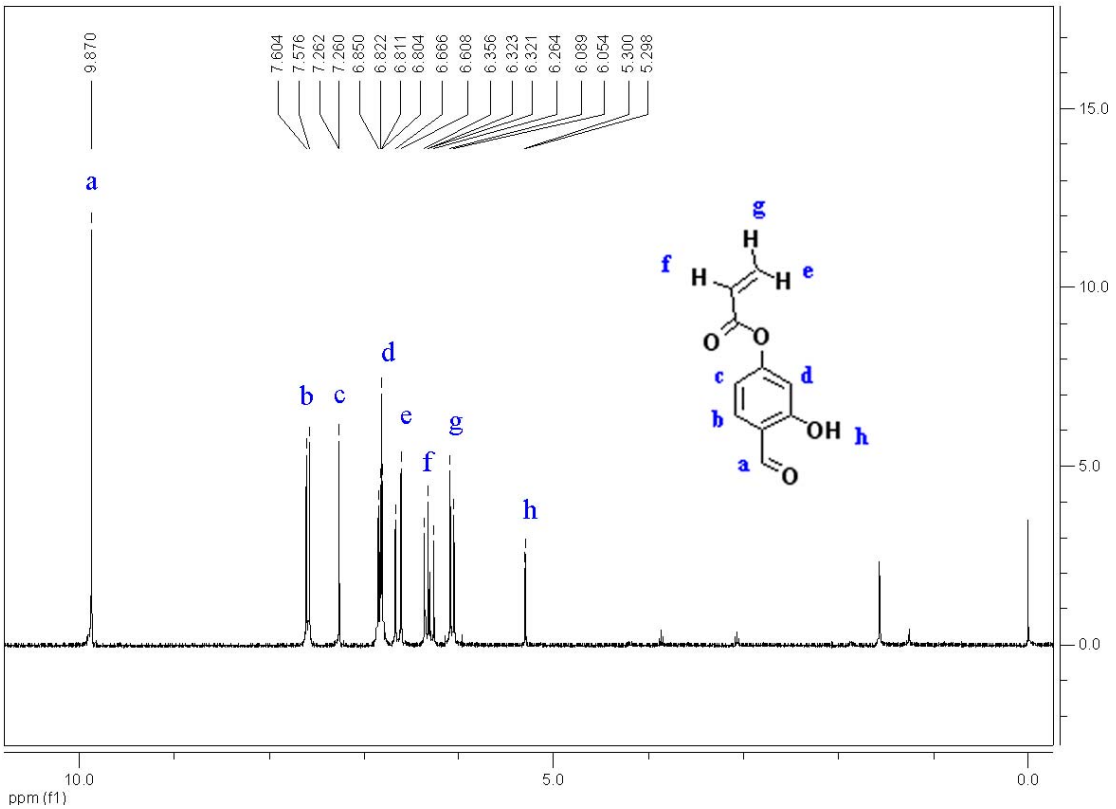

Fig. S1 ^{1}H NMR spectrum of AHPA.

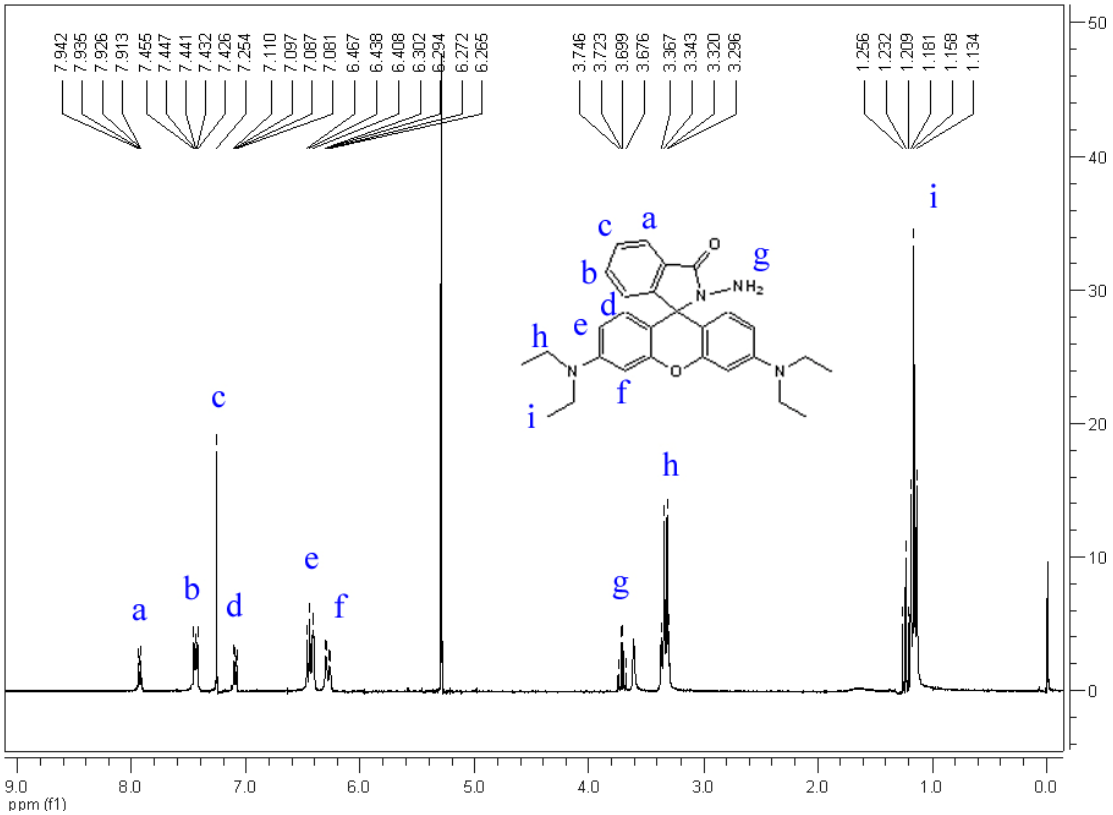

Fig. S2 ^{1}H NMR spectrum of RhB-hydrazine.

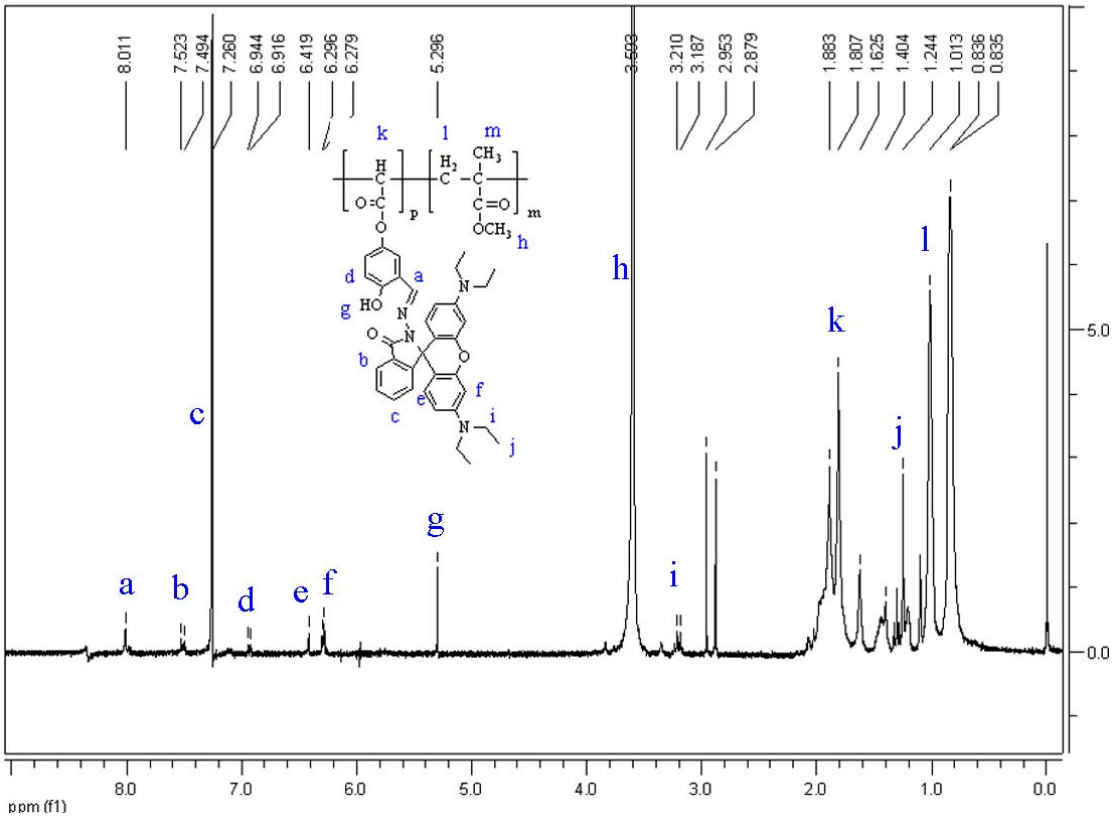

Fig. S3 ^{1}H NMR spectrum of poly(MMA-co-AHPA)/RhB in d6-DMSO at 25 ºC.

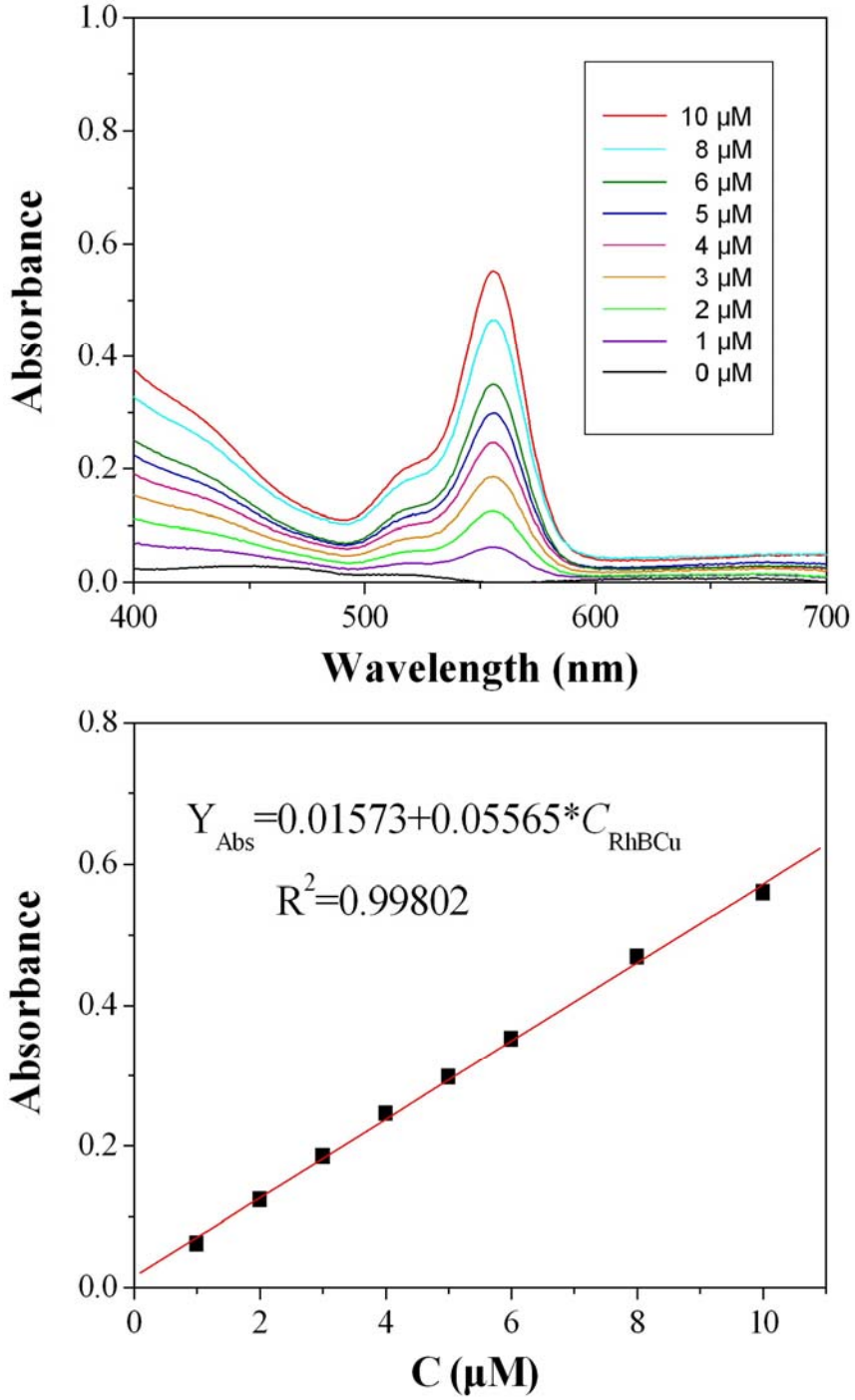

Fig. S4 Absorption spectra of monomer RhBCu (0, 1, 2, 3, 4, 5, 6, 8 and 10 μM) in DMF-H_2O solution and the linear fit of absorbance at λ_{abs} = 555 nm.

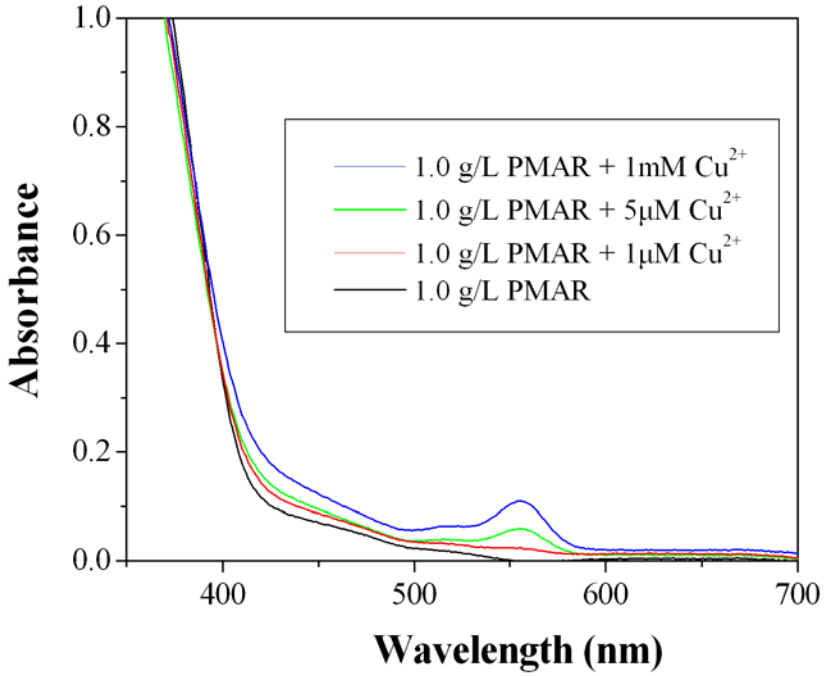

Fig. S5 Absorption spectrum change of poly (MMA-co- AHPA)/RhB 1.0 g/L with the addition of Cu^{2+} in DMF-H_2O solution.

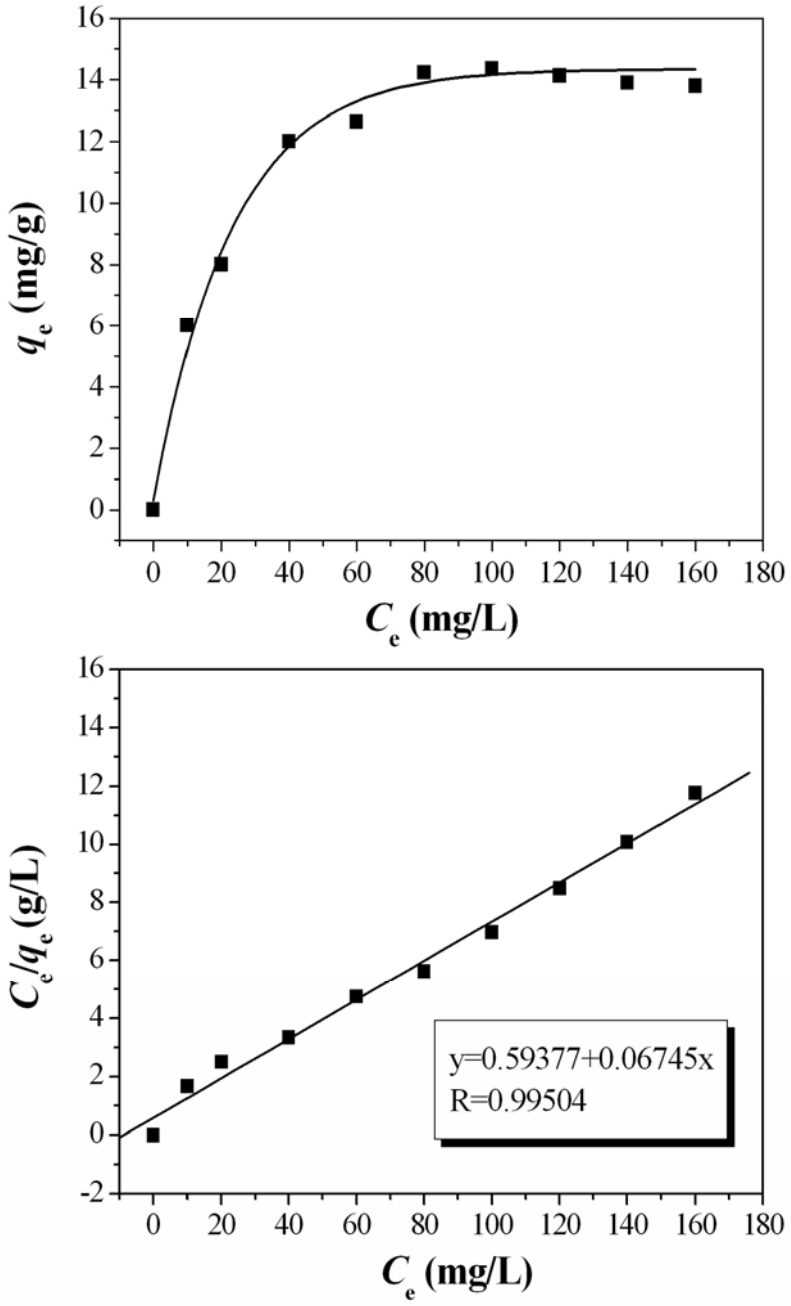

Fig. S6 (a) Adsorption isotherm and (b) Langmuir plot of Cu^{2+} on the PMAR nanofibrous film.

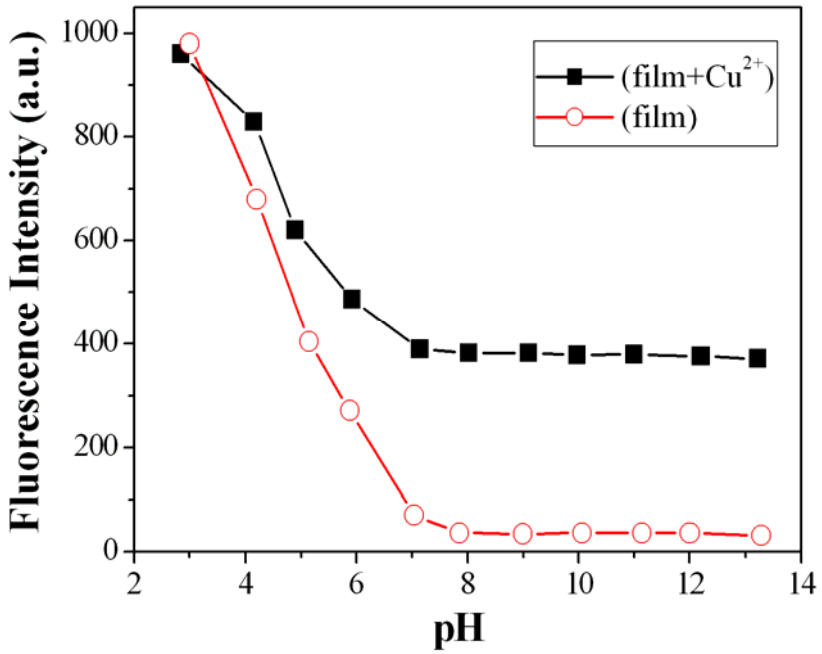

Fig. S7 Fluorescence emission of PMAR nanofibrous film in an ethanol-water (1:1, v/v) solution at different pH values, excitation wavelength was 500 nm. pH was adjusted by 75% $HClO_4$ and NaOH.

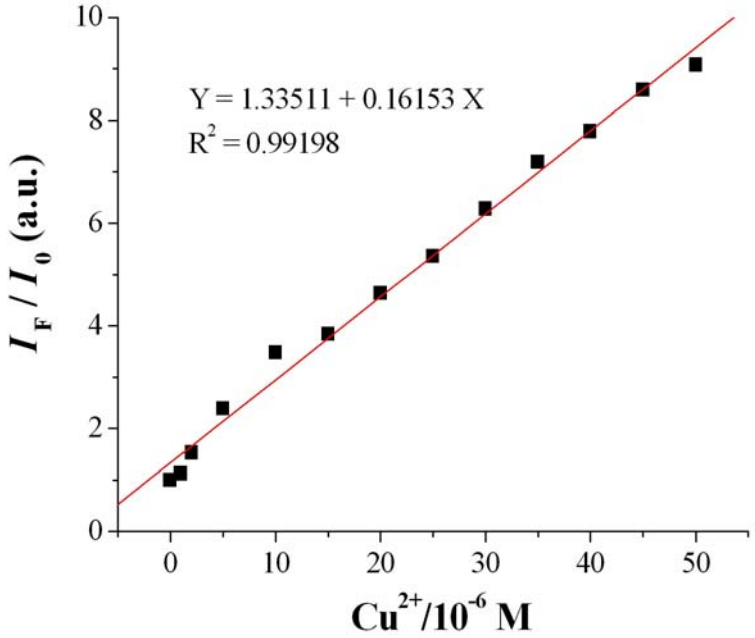

Fig. S8 Job plot: Fluorescence intensity at 557 nm of the film chemosensor versus increasing concentration of copper ion. (λ_{ex} = 520 nm.)

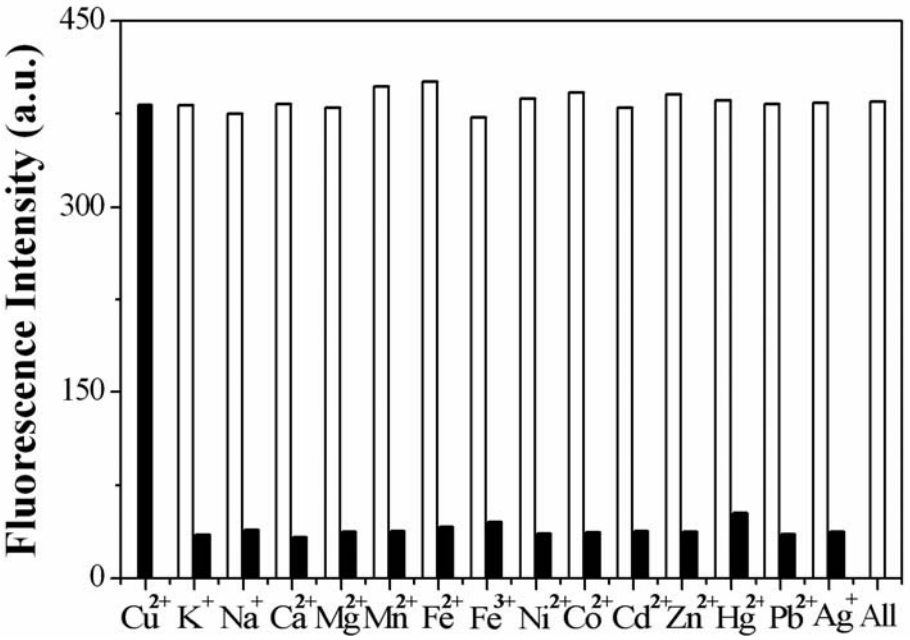

Fig. S9 Black bars: fluorescent emission response of the film in the presence of different metal ions in ethanol-water solution. White bars: fluorescent response of the film upon addition of 5.0×10^{-5} mol L^{-1} Cu^{2+} ions in the presence of 1.0×10^{-3} mol L^{-1} each of background metal ions.

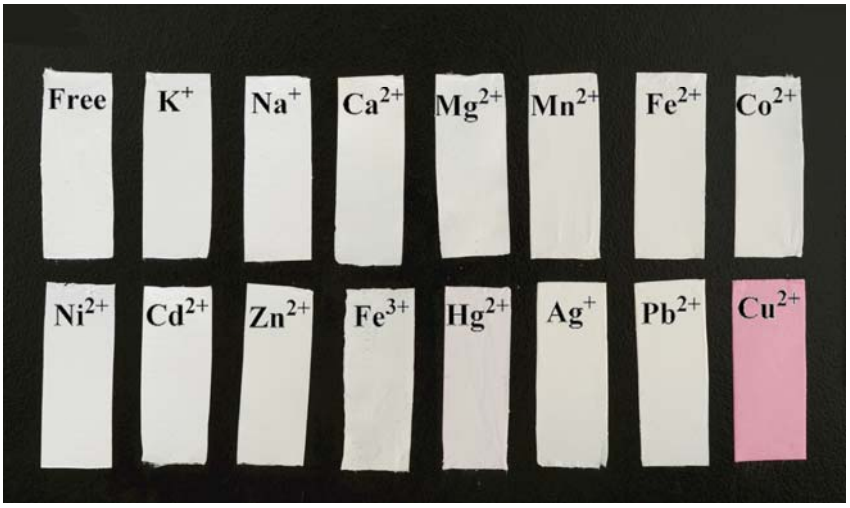

Fig. S10 Nanofibrous film in the presence of various metal ions (1.0×10^{-3} M except Cu^{2+} that is 5.0×10^{-5} M) in ethanol-water (1:1, v/v, pH=7.20) solution.

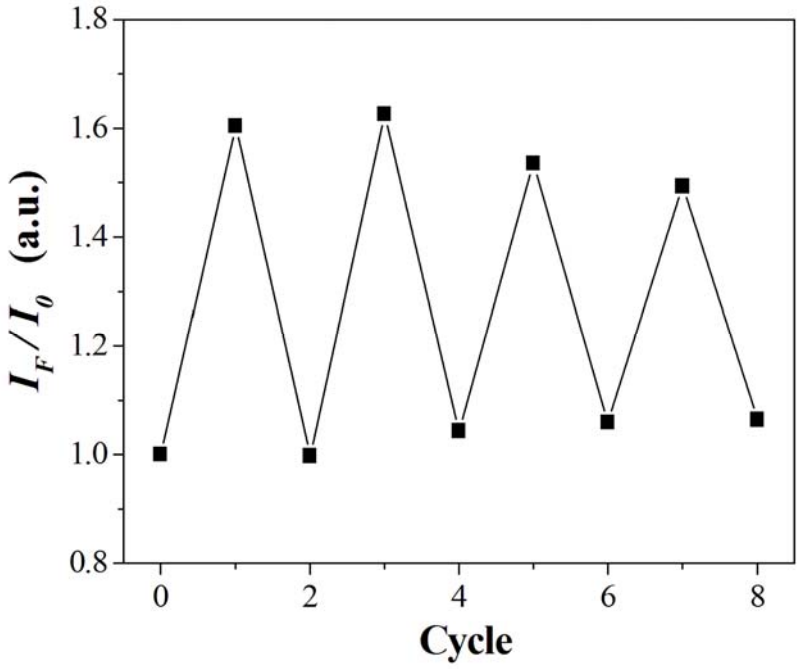

Fig. S11 Fluorescence intensity change for the PMAR nanofibrous film chemosensor after alternate treatment by aqueous solution of Cu^{2+} (1.5×10^{-6} mol L^{-1}) and EDTA.

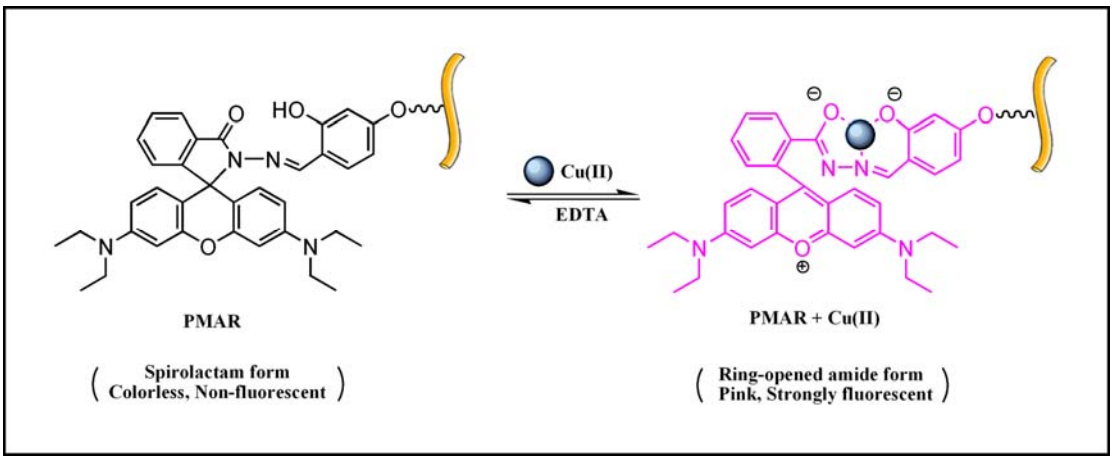

Fig. S12 The fluorescence/color change mechanism of PMAR in the presence of Cu^{2+}.

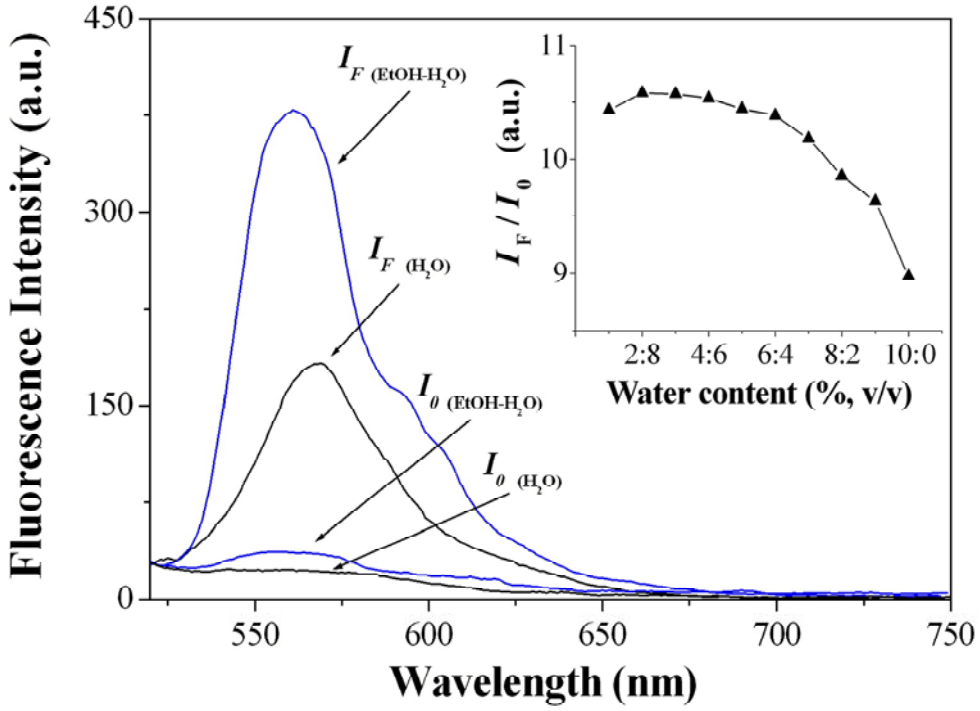

Fig. S13 Fluorescent spectra of the PMAR-Cu^{2+} complex nanofibrous film in pure aqueous solution and ethanol-water (1:1, v/v) solution. The inset shows effect of the water content on the fluorescence intensity of PMAR nanofibrous film in the presence and absence of Cu^{2+} ($[Cu^{2+}] = 2.0 \times 10^{-5}$ mol L^{-1}).

Table S1 Parameters for Cu^{2+} ions adsorption by PMAR nanofibrous film according to different equilibrium models

Langmuir isotherm constants			
Metal ion	K_L (L mg^{-1})	q_m (mg g^{-1})	R^2
Cu^{2+}	18.2335	14.3513	0.9901
Freundlich isotherm constants			
Metal ion	K_F	n	R^2
Cu^{2+}	2.1403	2.3140	0.9792
Tempkin isotherm constant			
Metal ion	ln$A$	B	R^2
Cu^{2+}	1.53534	2.4039	0.9543

4. References

[1] Q. Xu, J. Lu, X. Xia, M. Xiao, L. Wang, *J. Appl. Polym. Sci*. **2007**, *104*, 1285.

[2] K. Park, Y. M. Ju, J. S. Son, K. D. Ahn, D. K. Han, *J. Biomater. Sci., Polym. Ed*. **2007**, *18*, 369.

[3] T. G. Kim, D. S. Lee, T. G. Park, *Int. J. Pharm*. **2007**, *338*, 276.

[4] (a) Z. W. Ma, W. He, T. Yong, S. Ramakrishna, *Tissue Eng*. 2005, 11, 1149; (b) W. S. Li, Y. Guo, H. Wang, D. J. Shi, C. F. Liang, Z. P. Ye, F. Qing, J. Gong, *J. Mater. Sci*. **2008**, *19*, 847; (c) P. Ye, Z. K. Xu, J. Wu, C. Innocent, P. Seta, *Macromolecules*. **2006**, *39*, 1041.

[5] L. Fabbrizzi, M. Licchelli, A. Poggi, D. Sacchi, C. Zampa, *Polyhedron*. **2004**, *23*, 373.

[6] Y. Xiang, A. Tong, P. Jin, Y. Ju, *Org. Lett*. **2006**, *8*, 2863.

[7] K. Saeed, S. Haider, T. J. Oh, S. Y. Park, *J. Membr. Sci*. **2008**, *322*, 400.

[8] S. Deng, R. Bai, J. P. Chen, *Colloid Interface Sci*. **2003**, *260*, 265.

[9] Z. Xua, L Zhang, R. Guo, T Xiang, C Wu, Z. Zheng, F. Yang, *Sens. Actuators, B*. 2011, **156**, 546.

[10] Y. Xiang, A. Tong, P. Jin, Y. Ju, *Org. Lett*. **2006**, **8**, 2863.

[11] R. Tang, K. Lei, K. Chen, H. Zhao, *J. Chen, J Fluoresc*. **2011**, *21*, 141.

[12] P. F. Lee, C. T. Yang, D. Fan, J. J. Vittal, J. D. Ranford, *Polyhedron.* **2003**, *22*, 2781.

[13] P. Xi, J. Dou, L. Huang, M. Xu, F. Chen, Y. Wu, D. Bai, W. Li, Z. Zeng, *Sens. Actuators, B*. **2010**, *148*, 337.